



1 **Hydrological response in the Danube lower basin to some**
2 **internal and external climate forcing factors**

3
4
5
6
7
8
9
10
11

Ileana Mares¹, Venera Dobrica¹, Crisan Demetrescu¹, Constantin Mares²

¹ Institute of Geodynamics, Romanian Academy, Bucharest, Romania

² National Institute of Hydrology and Water Management, Bucharest, Romania

12
13
14
15
16
17
18
19
20
21
22
23
24
25
26
27
28
29
30
31
32
33
34
35
36

Abstract. Of the internal factors, we tested the predictors from the fields of precipitation, temperature, pressure and geopotential at 500hPa. From the external factors, we considered the indices of solar/geomagnetic activity. Our analysis was achieved separately for each season, for two time periods 1901-2000 and 1948-2000.

We applied developments in empirical orthogonal functions (EOFs), cross correlations, power spectra, filters, composite maps. In analysis of the correlative results, we took into account, the serial correlation of time series.

For the atmospheric variables simultaneously, the most significant results (confidence levels of 95%) are related to the predictors, considering the difference between standardized temperatures and precipitation (TPP), except for winter season, when the best predictors are the first principal component (PC1) of the precipitation field and the Greenland-Balkan-Oscillation index (GBOI). The GBOI is better predictor for precipitation, in comparison with North Atlantic Oscillation index (NAOI) for the middle and lower Danube basin.

The significant results, with the confidence level more than 95%, were obtained for the PC1-precipitation and TPP during winter/spring, which can be considered good predictors for spring/summer discharge in the Danube lower basin.

Simultaneous, the significant signal of geomagnetic index (aa), was obtained for the smoothed data by band pass filter. For the different lags, the atmospheric variables respond to solar/geomagnetic activity after about 2-3 years. The external signals in the terrestrial variables are revealed also by power spectra and composite maps. The power spectra for the terrestrial variables show significant peaks that can be associated with the interannual variability, Quasi-Biennial Oscillation influence and solar/geomagnetic signals.

The filtering procedures led to improvement of the correlative analyses between solar or geomagnetic activity and terrestrial variables, under the condition of a rigorous test of the statistical significance.

37
38

Keywords: NAO, GBOI, serial correlation, low and band pass filter, atmospheric blocking, Danube basin, climate changes

39
40
41

1 Introduction

42
43
44
45
46
47

Climatic system is a closed system, being influenced mainly by external factors, whose action is modulated by the internal mechanisms. Therefore, it is difficult to assess climatic system response to various external factors, the discrimination action of each is sometimes even impossible. The main external factors as is known are: solar activity in its various forms and the greenhouse gases that cause climate variability. The quantifying the



48 impact of each factor on the climate system is subject to various uncertainties. As shown in
49 Cubasch et al. (1997), as well as in Benestad and Schmidt (2009) is difficult to distinguish
50 between anthropogenic signal and the solar forcing in the climate change, especially if we
51 wanted to assess if the greenhouse or the solar forcing could be responsible for the recent
52 warming. An explanation of this shortcoming is related to the limits of simulation climate
53 models and lack of long data on many parts of the Earth, to estimate the impact of solar
54 activity.

55 In Brugnara et al. (2013) are reviewed recent studies on the impact of solar activity /
56 geomagnetic on the climate. After a statistical reconstruction of the main atmospheric fields
57 for more than 250 years, the authors performed an analysis of the solar signal of 11 years in
58 different terrestrial datasets, and they found that there was a robust response of the
59 tropospheric late-wintertime circulation to the sunspot cycle, independently from the date set.
60 This response is particularly significant over Europe.

61 There were many preoccupations regarding the impact of greenhouse gases, resulting
62 from climate modeling under various scenarios, on the water regime of the Danube. We
63 mention only some of these studies. In Mares et al. (2011, 2012) were processed climate
64 variables obtained from four global models of climate change: CNRM, ECHAM5, EGMAM
65 and IPSL, under A1B scenario. It was found for Danube lower basin, that the probability to
66 have extreme events (hydrological drought and great discharges) increases in the second half
67 of the 21st century comparing to the first half. A more complex methodology for post-
68 processing of outputs of climate models is found in Papadimitriou et al. (2016), where an
69 analysis of the changes in future drought climatology was performed for five major European
70 basins (including Danube) and the impact global warming was estimated.

71 Regarding internal factors that influence climate at regional or local scale, best known
72 index is related to the North Atlantic Oscillation (NAO). After Hurrell et al. (2003), NAO is
73 an internal variability mode of the atmosphere that depends exclusively on the dipolar
74 pressure distribution.

75 For the south - eastern European zone, only NAO is not a good enough predictor for
76 Danube discharge. Rimbu et al. (2002) showed that there is an out-of-phase relationship
77 between the time series of the Danube river discharge anomalies and the NAO index. Also,
78 Rimbu et al. (2005) was found that spring Danube discharge anomalies are significantly
79 related to winter Sea Surface Temperature (SST) anomalies. In Mares et al. (2002) was found
80 that NAO signal in climate events in the Danube lower basin is relatively weak, in
81 comparison with other regions.

82 However, we must note that NAO is a very good predictor for some regions. Thus, for
83 example NAOI is a significant predictor for : Seine river (Massey et al., 2010; El - Janyani et
84 al., 2012), northeastern Algeria (Turki, et al., 2016), southern Sweden (Drobyshev et al.,
85 2011), the northern Italy (Zanchettin et al., 2008).

86 The recent research (Valty et al., 2015) warns that for the predictor's selection such as
87 NAO, need to consider the dynamics of the total oceanic and hydrological system over wider
88 areas. In fact all climate system needs to be considered. In Hertig et al. (2015) are described
89 the mechanisms underlying the non-linearity and non-stationarity of the climate system
90 components, with a focus on NAO and the consequences of climate non-stationarities are
91 discussed.

92 In the present study, in comparison with the NAO influence on climate variables in the
93 Danube basin, we analysed the atmospheric index Greenland-Balkan-Oscillation (GBO),
94 which reflect the baric contrast between the Balkan zone and the Greenland zone. The GBO
95 index was introduced first time in Mares et al. (2013b) and in the present study it is shown in
96 detail, the GBOI informativity in comparison with NAOI, for the Danube basin.



97 Taking into account that solar activity plays an essential role in modulating the
98 blocking parameters with the strongest signal in the Atlantic sector (Barriopedro et al., 2008;
99 Rimbu and Lohmann, 2011), in the present paper we consider also, the indices of atmospheric
100 circulation of blocking type.

101 In this paper, except for the highlighting the atmospheric circulation of blocking type
102 taking into account the Quasi-Biennial Oscillation (QBO) phases and solar minimum or
103 maximum (number Wolf), we did not investigate any further interaction between internal and
104 external factors. This interaction was developed in other papers such as Van Loon and Meehl
105 (2014).

106 The main aim of our work was to select predictors from the terrestrial and solar
107 /geomagnetic variables with a significant informativity for predictand, i.e. discharge in the
108 Danube lower basin. We obtained this informativity by applying robust tests for the statistical
109 significance. Because the solar and geomagnetic variables, as well as the smoothing
110 procedures through various filters, respectively low pass filter and band pass filters applied in
111 this investigation, shows strong serial correlations, all correlative analyzes were performed
112 through rigorous testing of statistical significance. The number of observations was reduced to
113 the effective number of degrees of freedom, corresponding to the independent observations.

114 This paper is organized as follows: Sect. 2 shows data processed at regional scale (2.1)
115 and large scale (2.2), as well as the indices that define solar and geomagnetic activity (2.3).

116 In Section 3, we describe the methodology used. There are many investigations related
117 to solar / geomagnetic signal in the Earth's climate, some of them use smoothing of data, both
118 related to solar activity and the terrestrial variables. This smoothing induces a high serial
119 correlation, which produces very high correlations between time series analysis. Some authors
120 investigating these signals in the terrestrial variables take into account these large serial
121 correlations induced by these smoothing, others do not. Therefore in Sect. 3 we focused on
122 testing the statistical significance of solar / geomagnetic signal in climate variables, taking
123 into account the high autocorrelation induced by the smoothing processes. The confidence
124 level is found by robust method. We also briefly described the procedure of testing of
125 confidence levels of the peaks of the power spectra.

126 Section 4 contains the results and their discussion. Concerning the link between
127 atmospheric circulation at the large scale and the climate variables at local or regional scales
128 and described in 4.1, we demonstrated that GBOI is a predictor more significant than NAOI
129 for the climate variables in the Danube middle and lower basin. In 4.2, for the period 1901-
130 2000, we considered several predictors depending on climatic variables in the Danube basin,
131 as well the indices of large-scale atmospheric circulation and we tested predictor's weight for
132 the discharge in the lower basin. In subsection 4.3, are presented the results obtained from the
133 analysis of solar/geomagnetic signal simultaneously with the terrestrial variables (4.3.1) and
134 with some lags (4.3.2) and QBO role in modulating these signals (4.3.3). The conclusions are
135 presented in the Sect.5.

136

137

138 2 Data

139

140 2.1 Regional scale

141

142 Since the Danube discharge estimation has great importance for the economic sector
143 of Romania, in the present investigation we focused on predictors for Danube lower basin
144 discharge. The lower basin Danube discharge was evidenced by **Orsova station (Q_ORs)**,
145 located at the entrance of the Danube in Romania and representing an integrator of the upper
146 and middle basin. Our analysis was achieved separately for each season, for the two time



147 periods 1901-2000 and 1948-2000. For the period 1901-2000, in the Danube upper and
148 middle basin (DUMB), were considered fields of precipitation (PP), mean temperature (T),
149 diurnal temperature range (DTR), maximum and minimum temperatures (Tmx, Tmn), cloud
150 cover (CLD) at 15 meteorological stations upstream of Orsova. The selection of stations was
151 done according to their position on the Danube or on the tributaries of the river (Fig.1). The
152 values of monthly precipitation and temperature (CRU TS3.10.01) accessing
153 (<http://climexp.knmi.nl>). Data-sets are calculated on high-resolution (0.5 x 0.5 degree) grids
154 by Climatic Research Unit (CRU), and we selected for each station (with the respective
155 coordinators) the option “half grid points”.

156 The stations position in relation to Orsova is given in Figure 1. For each station was
157 calculated a simple drought index (TPPI), which is calculated by the difference between
158 standardized temperatures and precipitation. All analyses were achieved using the seasonal
159 averages for all variables considered in this study.

160

161

162 2.2 Large scale

163

164 In order to see the influence of large-scale atmospheric circulation on the variables at
165 the regional scale, we considered the seasonal mean values of sea level pressure field (SLP)
166 on the sector (50°W-40°E, 30°-65°N). We had to extract SLP data from the National Center
167 for Atmospheric Research (NCAR), (<http://rda.ucar.edu/datasets/ds010.1>). As mentioned in
168 the associated documentation, this dataset contains the longest continuous time series of
169 monthly girded Northern Hemisphere sea-level pressure data in the DSS archive. The 5-
170 degree latitude/longitude grids, computed from the daily grids, begin in 1899 and cover the
171 Northern Hemisphere from 15°N to the North Pole. The accuracy and quality of this data is
172 discussed in Trenberth and Paolino (1980).

173

174 We found a new index started from tests achieved using correlative analysis between
175 the first principal component (PC1) of the Empirical Orthogonal Functions (EOFs)
176 development of the precipitation field defined at 15 stations from Danube basin and each grid
177 point where SLP is defined. By determining the centers of inverse correlation nuclei (positive
178 and negative) and by considering the normalized differences between SLP at Nuuk and Novi
179 Sad (Fig.2), we obtained this index, which we called *Greenland-Balkan-Oscillation index*
180 (GBOI). This index was introduced by Mares et al. (2013b) and tested in the previous works
181 of the authors (Mares *et al.*, 2014a, 2015a,b, Mares et al., 2016a,b).

182 The NAOI were download from <http://www.ldeo.columbia.edu/res/pi/NAO/>

183 For 1948-2000 period beside of variables taken over 1901-2000, we considered and
184 blocking type indices.

185 For the geopotential at 500 hPa (1948-2000) provided by *British Atmospheric Data*
186 *Centre (BADC)* three sectors were taken into account: Atlantic-European (AE) on the domain
187 (50°W- 40°E; 35°N - 65°N), Atlantic (A) defined in (50°W - 0°, 35°N - 65°N) and European
188 (E) in the region (0° -40°E; 35°N - 65°N).

188

189 2.3 Solar / geomagnetic data

190

191 For this 100 year period the solar/geomagnetic activities were quantified by Wolf
192 number and *aa* index. For the period 1948-2000, solar forcing is quantified by the 10.7 cm
193 solar flux instead of Wolf number. Since the 10.7cm flux is a more objective measurement,
194 and always measured on the same instruments, this proxy "sunspot number" should have a
195 similar behaviour but smaller intrinsic scatter than the true sunspot number
196 (ftp://ftp.ngdc.noaa.gov/STP/SOLAR_DATA/). The values for the Quasi-Biennial Oscillation



197 (QBO) were downloaded from Free University of Berlin (<http://www.geo.fu-berlin.de/met/ag/strat/produkte/qbo/qbo.dat>).

198

199

200 3 Methodology

201

202 The time series of the variables considered in the 15 stations were filtered by the first
203 principal component (PC1) of empirical orthogonal functions (EOFs) development.

204 The analyse of the low frequency components of the atmosphere, based on
205 decomposition in multivariate EOF (MEOF), was used by the authors of the present paper in
206 Mares et al. (2009, 2015, 2016a, b).

207 The 500 hPa geopotential field was filtered by blocking index (I_B) as is described in
208 Lejenas and Okland (1983). Such a blocking event can be identified when the averaged zonal
209 index computed as the 500-hPa height difference between 40° and 60° N, is negative over 30°
210 in longitude. Taking into account the above definition, in the present study, we calculated for
211 each longitude λ , three indices for the regions: Atlantic-European (AEBI), Atlantic (ABI) and
212 Europe (EBI) after the formula:

213

$$214 \quad IB(\lambda) = \Phi(\lambda, 57.50 N) - \Phi(\lambda, 37.50 N) \quad (1)$$

215

216 where Φ is the 500 hPa geopotential field, and blocking index I_B is a mean for λ longitudes of
217 $IB(\lambda)$. In our case IB positive reflects a blocking type circulation.

218 In the preprocessing analyses, low and band pass filters were applied.

219 **Low pass filters** were applied to eliminate oscillations due to other factors as El
220 Niño–Southern Oscillation (ENSO) than the possible influence of solar/ geomagnetic
221 activities. The Mann filter (Mann, 2004, 2008) was applied with three variants that eliminate
222 frequencies corresponding the periods lower than 8, 10 and 20 years.

223 Besides the low pass filters specified above, which was applied only to the terrestrial
224 fields, **the band pass filters** were applied both to the terrestrial and solar or geomagnetic
225 variables. The band pass filters were of the Butterworth type, and the variables have been
226 filtered in the 4–8, 9–15 and 17–28 years bands.

227 In Lohmann et al. (2004) the solar variations associated with the Schwabe, Hale, and
228 Gleissberg cycles were detected in the spatial patterns in sea-surface temperature and sea-
229 level pressure, using band pass filters with frequencies appropriate to each of the solar cycles.
230 Significant correlations between global surface air temperature and solar activity were
231 obtained by Echer et al. (2009), applying wavelet decomposition with different the band
232 frequencies.

233 As is known in the literature, the response of climate variables to the
234 solar/geomagnetic activity is evidenced not only simultaneously but also certain differences,
235 we performed cross - correlation with a lag of 5 years. Explanation of the physical mechanism
236 of correlations with certain lags between solar activity and climate variables is found in Gray
237 et al. (2013) and Scaife et al. (2013).

238 In order to find the significance level of the correlation coefficient, we have to take
239 into account the fact that by the smoothing both terrestrial and solar/ geomagnetic variables
240 present a serial correlation. In this case, we have to estimate the equivalent sample size (ESS).
241 There are more methods to find the correlations statistical significance among the series pairs
242 presenting serial correlations. A part of these methods are present in Thiebaut and Zwiers
243 (1984), Zwiers and Storch (1995), Ebisuzaki (1997).

244 In Mares et al. (2013a), the procedure described by Zwiers and Storch (1995) for ESS
245 estimation was applied in order to estimate the statistical significance of the climatic signal in
246 sea level pressure field (SLP) in 21st century in comparison with 20-th century.



247 In the present analysis, in order to find the ESS, namely the *number of effectively* independent
248 observations (N_{eff}) is applied a simple formula, which is appropriate for the correlations
249 involving smoothed data (Bretherton et al., 1999).

$$250 \quad N_{eff} = N \frac{(1 - r_1 r_2)}{(1 + r_1 r_2)} \quad (2)$$

251 where r_1 and r_2 are the lag-1 autocorrelation coefficients corresponding to the two time
252 series correlated and N number of the observations.

253 In the next phase, the t-statistic is used to test the statistical significance of the
254 correlation coefficient:

$$255 \quad t = |r| [(N_{eff} - 2)/(1 - r^2)]^{1/2} \quad (3)$$

256 In equation (3), r is the correlation coefficient between the two variables and N_{eff} is
257 effective number used in the testing procedure.

258 According to von Storch and Zwiers (1999), the null hypothesis $r = 0$, is tested by
259 comparing the t value in equation (3) with the critical values of t distribution with $n_e - 2$
260 degrees of freedom.

261 The correlated time series must have a Gaussian distribution. For this reason in the present
262 study we have also applied and the nonparametric Kendall correlation coefficient, which
263 measures of correlation of the ranked data. Applying the algorithm described in Press et al.
264 (1992), correlation values and corresponding significance p-levels are obtained. A comparison
265 between the Pearson and Kendall correlation coefficients is found in Love et al. (2011),
266 where the statistical significance between sunspots, geomagnetic activity and global
267 temperature, is tested.

268 Among the statistical methods that might be used to test solar or geomagnetic
269 activity signal in the climatic variables, in this study we will take into account also on testing
270 the statistical significance of the amplitude of the power spectra in time series. Testing the
271 statistical significance of the peaks obtained from an analysis of a time series by power
272 spectra is usually done by building a reference spectrum (background) and comparing the
273 amplitude spectrum analyzed time series based spectrum amplitudes. This spectrum is a series
274 based on white noise or most often a red noise series (Ghil et al. 2002, Torrence and Campo,
275 1998). At first all amplitudes above the background noise amplitudes are considered
276 significant. But to test how significant are these peaks are testing their statistical significance
277 compared with different levels of significance desired.

278 A significance test requires null hypothesis significance. For spectral analysis, the null
279 hypothesis is that the time series has no significant peak and spectral estimation differs from
280 the noise spectrum (background). Rejection of the null hypothesis means accepting peaks of
281 the spectrum series of observations that exceed a certain level of significance. As shown in
282 Mann and Less (1996) theoretical justifications exist for considering red noise as noise
283 reference (background) for climate and hydrological time series.

284 The power spectra achieved in this study were estimated by multitaper method (MTM)
285 (Thomson, 1982, Ghil et al., 2002, Mann and Less (1996)). The MTM procedure is a
286 nonparametric technique that does not require a priori a model for the generation of time
287 series analysis, while harmonic spectral analysis assumes that the data generation process
288 include components purely periodic and white noise which are overlapped (Ghil et al., 2002).

289 In Mares et al. (2016), more practical details were given on estimating background
290 noise and significance of power spectra peaks, for the applications referring to the influence of
291 the Palmer drought indices in the Danube discharge.

292

293

294



295 **4 Results and discussions**

296

297

298

299

297 **4.1 Connection between atmospheric circulation at the large scale and climate** 298 **events at regional or local scale**

300

301

302

303

304

The atmospheric circulation at the large scale is quantified in this paragraph by North Atlantic Oscillation index (NAOI), Greenland Balkan Oscillation Index (GBOI) and indices that highlight the blocking type circulation. The direct impact of NAO is less obvious than GBO impact for the surrounding areas of the lower Danube basin as revealed in this study and in previous investigations (Mares et al., 2013b, 2014, 2015a,b 2016a,b).

305

306

307

308

The high correlations between GBOI and precipitation are stable over time (Table 1). From how GBO and NAO indices are defined, they have opposite signs. Temporal evolution for winter of the first principal component (PC1) for the precipitation in the Danube basin in comparison with GBOI values is given in Fig.3.

309

310

311

312

The details on the stations are given in Fig.4, where are presented the correlation coefficients between winter precipitation at 15 stations and NAOI and GBOI for two periods 1916-1957 and 1958-1999. From this figure, it is clear that the GBOI signal is stronger than NAO signal, except for the first stations located in the upper basin of the Danube.

313

314

315

316

317

318

319

320

321

322

323

324

325

326

327

Since the Danube discharge estimation in spring season with some anticipation has great importance for the economic sector of Romania, the best predictors at the large scale for Orsova discharge in spring, with one season anticipation (winter) were revealed, with high confidence level (> 99%): GBOI as well as the atmospheric circulation of blocking type, quantified by European blocking index (EBI). The Figure 5 shows spring Orsova discharge (standardized) in comparison with European blocking index ($R = -0.54$) and GBOI ($R = 0.53$) for winter in the period 1948-2000. The opposite signs of the Orsova discharge correlations with EBI and GBOI are due to the definitions of the two indices. The negative correlations between discharge and EBI can be explained as follows. As shown in Davini et al. (2012), the midlatitude traditional blocking localized over Europe, uniformly present in a band ranging from the Azores up to Scandinavia, leads to a relatively high pressure field in most of Europe. This field of high pressure, which defines a positive blocking index, and is not favorable for precipitation, leads to in low discharge of the Danube at Orsova. A positive correlation coefficient between the Danube discharge at Orsova and GBOI, means that a positive GBO index lead to a low pressure in the Danube basin area and therefore a high discharge.

328

329

330

331

The role of the atmospheric circulation of blocking type on events in the Danube Basin is described in many papers, including Mares et al. (2006), Blöschl et al. (2013).

332

333

334

332 **4.2 Testing predictor variables for estimating the discharge in the Danube lower basin** 333 **(1901-2000)**

335

336

337

338

339

340

341

342

343

344

To underline the contribution of the nine predictors, defined at the 15 stations in the Danube basin, described in Section 2, we represented in Figure 6 the correlation coefficients between Danube discharge at Orsova (lower basin) and these predictors for each of the four seasons. PC1 in Fig. 6 represents the first principal component of EOFs development of the respective fields. If we take into account the confidence level at 99%, of correlation coefficients for 100 values, it should exceed 0.254. There are many predictors that are statistically significant at this level of confidence, but we take into consideration only those having the highest correlation coefficients. As can be seen from Figure 6, the greatest contribution to the Danube discharge in seasons of spring, summer and fall, brings the drought index (depending on precipitation and average temperature), with the correlation



345 coefficients (r) of -0.450 - 0.730 for spring and summer and respectively -0.700 for fall. In
346 winter season, the highest contribution to the discharge in lower Danube basin, it has
347 precipitation field in the upper and middle basin ($r = 0.500$), followed by GBOI ($r = 0.430$).
348 Also, it is revealed that for the spring season, where contribution drought index TPPI is
349 lower than in summer and autumn season, the GBOI and DTR can be considered good
350 predictors with $r = 0.420$ and respectively -0.417 .

351 Regarding consideration of the predictors with some anticipation to the Danube
352 discharge, the significant results obtained with an anticipation of a season, are presented in the
353 Fig. 7. For spring, the best predictor is clearly drought index (TPPI), taken in winter ($r = -$
354 0.62), and also for summer discharge, TPPI in spring is a significant predictor ($r = -0.55$), but
355 quite closely related this is the spring precipitation field quantified by PC1 ($r = -0.53$).

356 The results obtained in this study are consistent with those of Mares et al. (2016a),
357 where that the Palmer drought indices were found good predictors for the discharge in lower
358 basin.

359

360

361 **4.3 Solar/geomagnetic signal in the climate fields in Danube basin**

362

363 Solar activity was represented by Wolf numbers for the period 1901-2000 and by 10.7-
364 cm solar flux for the period 1948-2000. Although the solar flux is closely correlated with
365 Wolf numbers, these values are not identical, the correlation coefficient varying with the
366 season (0.98 - 0.99). The geomagnetic activity was quantified by aa index for the two periods
367 analyzed (1901-2000 and 1948-2000). Regarding the link between solar activity and
368 geomagnetic, details are found in Demetrescu and Dobrica (2008).

369 Solar/geomagnetic signal was tested by: correlative analyses (simultaneous and cross
370 correlation), composite maps and spectral analyses. Before correlative analysis, data were
371 filtered using low and band pass filters for the terrestrial variables and only band pass filters
372 for the solar / geomagnetic indices.

373 Related to the low pass filter, the Mann filter (Mann, 2004, 2008) was applied with
374 three variants that eliminate frequencies corresponding the periods lower than 8, 10 and 20
375 years. The analysis revealed that from the three variants, time series cutoff 8, responded best
376 to variations in solar / geomagnetic activities.

377 In many investigations, significant solar signal in the terrestrial variables, have been
378 obtained applying band pass filters, for isolating the frequency bands of interest (Lohmann et
379 al., 2004, Dima et al, 2005, Prestes et al. 2011, Echer et al. 2012, Wang and Zhao, 2012).

380 In the present study we apply a band pass filter with the three frequency bands: (4-
381 8yr), (9-15yr) and (17-28 yr). Because after the filtering process, the time series show a
382 strong autocorrelation, to test the statistical significance of the link between the terrestrial and
383 solar variables, we use the t -test, which takes into account the effective number of
384 independent variables and the correlation coefficient between two series. The effective
385 number is determined in function of the serial correlations of the two series analyzed. Details
386 are given in Section 2. The most significant results were obtained for the filtered terrestrial
387 variables, taken with some lags related to solar or geomagnetic activity.

388

389 **4.3.1 Simultaneously signal**

390

391 The Table 2 presents some of the results that have a confidence level higher or least of
392 95%, which worth to be taken into account for the analysis period of 100 years (1901-2000).
393 Here are presented only the results simultaneously for three categories of data: non-filtered
394 (UF), smoothed by low pass filter (LPF), eliminating, the periods less than or equal to 8 years,



395 only for terrestrial variables, and band pass filter (BPF) applied for both time series (terrestrial
396 and solar / geomagnetic indices).

397 Since not all variables have a normal distribution, the Kendall's coefficient was
398 associated Pearson's coefficient. The nonparametric Kendall coefficient is valid for time
399 series that do not have a normal distribution. There are cases when the difference between the
400 two correlation coefficients is relatively high and this difference may be due to statistical
401 distribution that deviates from normal.

402 As can be seen from Table 2, smoothing time series lead to improved correlation
403 coefficients, the most significant results were obtained by band-pass filter with frequency
404 corresponding to 9-15 yr. Also, tests were achieved and 17-28 yr, but although, highest
405 correlation coefficients were obtained, it is difficult to take a decision, because the effective
406 number is very small (about 5 years), due to serial correlation very high, caused by such
407 filters. For such filtering are necessary much larger sets of data. An example is given in Tab. 2
408 to test the correlation between the GBOI and Wolf number during fall season.

409 The results presented in the Table 2, related to the significant correlations indicated by
410 Pearson coefficients (r), are supported by Kendall correlation coefficients (τ), and their levels
411 of significance (p). Bold lines means there are at least two situations for the same season
412 (filtered or unfiltered data) having a significantly CL.

413 As can be seen from Table 2, highest correlations with aa , were obtained during the
414 summer season with $r = 0.796$ for temperature and with $r = -0.721$ for precipitation, for a
415 smoothing by a BPF with the band (9-15yr). Also, in summer, it is worth to mention the aa
416 signal in drought index (TPPI) with the correlation is 0.787, corresponding filtering with (9-
417 15 yr). From the definition of this index, it reflects the behavior of both temperature and
418 precipitation, but the sign is given by temperature. It can be noting that drought index TPPI,
419 which is a combination of temperature and precipitation, responds better to signal aa ,
420 compared to PC1_PP. Therefore, a geomagnetic activity maximum (minimum) determines a
421 situation of drought (wet) in the Danube basin during spring and summer.

422 Regarding solar activity signal in temperatures and precipitation, the highest
423 correlation coefficients were found for the fall season (0.699) and respectively for spring (-
424 0.538) in the band filter (9-15 yr). From the Table 2, are observed correlations with the
425 number Wolf, with a particularly high confidence level (> 99%) in the case of considering
426 time series smoothed by the band (4-8 yr), as atmospheric circulation index GBOI (summer
427 and winter).

428 The results obtained in the present investigation, referring to the temperature and
429 precipitation variables are in accordance with the ones from Dobrica et al. (2009, 2012),
430 where have been analysed the annually mean of long time series (100–150 years) for the
431 temperature and precipitation records from 14 meteorological stations in Romania. There are
432 some differences, because in this investigation, fields of temperature and precipitation are
433 taken on another area, smoothing procedures are different and the analysis is done on each
434 season separately. However, the correlations with the geomagnetic aa index and Wolf
435 numbers have the same sign, ie positive for temperatures and, negative for precipitation
436 respectively.

437 Reducing the number of effective observations, when is applied a smoothing, is
438 discussed in Palamara and Bryant (2004), where they test the statistical significance of the
439 relationship between geomagnetic activity and the Northern Annular Mode.

440 Although the results obtained here by the BPF shows the largest correlation
441 coefficients, however those obtained by BPF (9-15) must be analyzed together with results
442 obtained by other filters. An example is the solar signal, quantified by Wolf number, in the
443 drought index (TPPI), for which in the spring, unfiltered data, filtered by the low pass filter,
444 and those by BPF (4-8 and 9-15) indicate correlations with confidence level higher than 90%,



445 it means that significance of the correlation in this case, does not depend on the time series
446 size.

447 Taking into account both signals of the geomagnetic and solar activity, we can notice
448 that during spring, TPPI has the best respond for unfiltered or filtered time series.

449 Considering the importance of the Danube discharge in our study, we analyze solar /
450 geomagnetic signals in this variable. Thus, the *aa* signal in Danube discharge at Orsova
451 (Q_ORs), is seen as the most significant, during the summer season with correlation
452 coefficient $r = - 0.656$. But considering our criteria above enumerated, ie significant
453 correlations in at least two cases, it is clear that we must focus on the discharge behavior in
454 fall (Table 2), for which the smoothing by LPF and BPF (9-15) lead to the significant
455 response to *aa* impulse.

456 In the following, we present results obtained by analyzing the terrestrial and solar or
457 geomagnetic data for the period 1948-2000. Although the time series are relatively short, was
458 considered this period because some of the atmospheric variables, as indices that define the
459 type blockage 500 hPa, are available only in 1948. Also 10.7 cm solar flux that defines more
460 clearly solar activity is just beginning in this period. In addition, we wanted to see if it
461 improves the relationship between the terrestrial and solar indices, taking separately the years
462 with positive or negative phase of Quasi-Biennial Oscillation (QBO).

463 In the Table 3 are presented the correlation coefficients, with a high confidence level
464 (>95%), obtained from the simultaneous correlative analyzes between terrestrial variables and
465 gemagnetic (*aa*), and solar activity (flux 10.7cm) indices on the other hand. It is observed that
466 due to short time series, the smoothing by the band pass filter (9-15), although leads to the
467 correlation coefficients with high confidence level, the number of degrees of freedom is quite
468 small.

469 For this period of 53 years (1948-2000), the smoothing by BPF with the band (4-8 yr)
470 appears most appropriate, especially for highlighting solar signal, where all three blocking
471 indices considered in this paper, respond significantly to the solar impulse.

472 The solar or geomagnetic signals in the terrestrial variables can be emphasized also by
473 the periodicities estimation by means of the power spectra. In the present study the power
474 spectra were estimated by means of multitaper method (MTM). For the time series of
475 unfiltered European blocking index (EBI) during winter, the power spectra given in the Fig.8a
476 reveals that the most significant periodicity is related to QBO (2.4 years), and with an
477 approximately 90% confidence level are the peaks at 10.7 and 14.2 years, which may be
478 linked to 11-year solar/geomagnetic cycle. In Fig. 8b, which represents the power spectrum
479 for EBI in the spring, the only significant peak with a confidence level of 95% is situated at
480 10 years. This is consistent with the results shown in Table 3, where during spring, the time
481 series of blocking index EBI, both unfiltered and filtered by the band pass filter (4-8) have
482 significant correlations with the *aa* geomagnetic index. Also, in winter (Fig. 8a), the EBI's
483 response to solar activity, quantified by the Wolf number, is statistical significant with CL
484 almost 99%. If we take only spring season, the best significant peak related to QBO (Fig. 8c)
485 is found in blocking index over Atlantic European region (AEBI).

486 Graphical representation of unfiltered time series was given to see whether the there
487 are solar/ geomagnetic signals in the original series. The power spectra of the filtered series
488 were not shown, because these series show peaks corresponding to the frequencies remaining
489 after filtering procedure.

490 Regarding the period of 53 years (1948-2000), significant signals of the solar activity
491 quantified by solar flux 10.7cm were obtained for spring and summer in the Danube discharge
492 at Orsova (Q_ORs), with different lags, especially to a delay of two years, where both
493 unfiltered and filtered time series, indicate statistically significant correlations.



494 Like in the GBOI case, the discharge is inversely, but well correlated with solar
495 activity. In Fig. 10a, correlation coefficients are shown at the lags 1-5 for three series,
496 unfiltered (UF), smoothed by low pass filter (LPF) and the band pass filter (9-15). It can be
497 observed that, if for the unfiltered data, the signal is significant at the lag 1 and 2, for the data
498 smoothed by BPF, this signal is at the lags 2, 3 and 4. Taking into account the LPF result,
499 can be considered the most significant result at the lag 2 years. In the Fig. 10b have been
500 shown the coherent time evolutions of the solar flux and discharge, smoothed by BPF (9-15)

501 with a lag of three years, where, the correlation coefficient is highest (-0.769) and CL is 99%.
502 From the above results, we can highlight that the Danube discharge in the lower basin,
503 at the 2 or 3 years during spring and summer, after a maximum (minimum) solar, will be
504 lower (higher).

505 A different response to solar activity was found in the time series of the index that
506 defines a atmospheric circulation of blocking type over Atlantico-European region, for the
507 period 1948-2000, during the winter season. As can be seen in Fig. 11, the response this index
508 to the solar activity is significant with a delay of two years and three years compared to the
509 solar flux. It is worth noting that in this case, the filtering process does not lead to an
510 improvement of the significance of the correlation, even if its value increases. Thus it is
511 necessary a rigorous test for correlation's significance, especially for data smoothed.

512 Therefore, we might conclude that about 2-3 years after producing a maximum (minimum)
513 solar, winter, atmospheric circulation of blocking type is enhanced (weakened) over the
514 Atlantico-European region.

515

516

517 4.3.3 QBO role

518

519 Regarding QBO influence on the relationship between solar activity and terrestrial
520 parameters, there are several investigations (Van Loon and Labitzke, 1988; Bochníček et
521 al.1999, Huth et al., 2009), which demonstrated that QBO phase is very important for
522 emphasizing these links. We see in QBO mainly an important modulator of the impact of
523 solar activity on the phenomena of the lower troposphere. To test these findings, in this paper,
524 the years with east QBO phase, during winter months have been selected, and were made
525 correlations between solar flux and more terrestrial variables. Winter, from the atmospheric
526 indices of blocking type at 500 hPa, best response at the QBO signal, was found in the
527 blocking over the European sector (EBI), with power spectrum shown in Fig. 8a. But the
528 correlation coefficient between the solar flux and the unfiltered EBI during winter, for all
529 those 53 years, is 0.15 and not is statistically significant. By selecting only the years with
530 QBO in the east phase in the winter months (34 cases), the correlation coefficient is 0.32 at
531 the confidence level around 95%. It is interesting that although the power spectrum (Fig. 8a)
532 highlights significant peaks related to the QBO (2.4 and 2.7ani), the correlation coefficient
533 between EBI and QBO is insignificant. This suggests that the spectral representation is very
534 useful in time series analysis and the QBO phases modulate the connection between solar
535 activity and blocking circulation.

536 It is enlightening solar impact (by flux) on atmospheric circulation in the lower troposphere,
537 during the east phase of QBO, when the solar maximum is associated with blocking event over the
538 Northern Atlantic and north-western Europe (Fig. 12a), and a geopotential with a opposite
539 distribution that occurs during the solar minimum. (Fig. 12b).

540 The advantage of the composite maps, used to outline the response to the solar signal, is
541 shown in Sfıca et al. (2015), which specifies that through these composite maps, nonlinearities are
542 taken into account, compared to using linear methods.



543 Our findings, presented in the Fig. 12, are in concordance with Barriopedro et al. (2008),
544 namely, QBO is a modulator of the of the atmospheric circulation transformation from a blocking
545 type circulation to a zonal one and vice versa, under the solar impact.

546 We mention that in the period 1948-2000 were recorded 34 months of winter (DJF) in which
547 occurred east QBO phase and the solar flux has produced in the lower troposphere an atmospheric
548 blocking events, or a zonal atmospheric circulation, at middle and higher latitudes, depending on the
549 state of maximum or minimum solar activity, respectively.

550

551

552 **5 Conclusions**

553

554 In the present investigation, we focused on finding predictors for the discharge in the
555 Danube lower basin, which present a high level of statistical significance.

556 In the first part of the paper we tested the predictors for the discharge, from the fields
557 of temperature, precipitation, cloud cover in the Danube basin, and indices of atmospheric
558 circulation over the European Atlantic region. For climate variables defined in the Danube
559 basin, as predictor we used only the first principal component (PC1) of the EOFs
560 decomposition and a drought index (TPPI) derived from the standardized temperature and
561 precipitation.

562 The atmospheric circulation has been quantified by Greenland Balkan Oscillation
563 (GBO) and North Atlantic Oscillation (NAO) indices and the blocking type indices. The
564 analysis was performed separately for each season and on the two period (1901-2000) and
565 (1948-2000).

566 Main statistically significant results for this part of our research are the following:

- 567 1. The correlative analyzes simultaneously for each season, revealed that, except for
568 the winter season, drought index (TPPI) has the highest weight to the discharge
569 variability in the lower basin of the Danube.
- 570 2. Testing the predictors, in order to see their predictive capacity, with a lag of
571 several months in advance of discharge, concluded that TPPI in winter and spring
572 is a good indicator for the Danube discharge in spring and summer respectively.
- 573 3. We demonstrated that for the winter, GBOI has an influence on the climate
574 variables in the Danube middle and lower basin more significant than NAOI.
- 575 4. Analysis for the period 1948-2000, reveals that in winter, the GBOI weight for the
576 Danube discharge is similar to those of the blocking index over the European
577 sector.

578 In the second part of the paper, we focused on solar/geomagnetic signals in the
579 terrestrial variables. Because the solar and geomagnetic variables as well as the smoothing
580 procedures through various filters, respectively low pass filter and band pass filters applied in
581 this investigation, shows strong serial correlations, all correlative analyzes were performed
582 through rigorous testing of statistical significance. The number of observations was reduced to
583 the effective number of degrees of freedom, corresponding to the independent observations.

584 The filtering procedures led to improvement of the correlative analyses between solar or
585 geomagnetic activity and terrestrial variables, under the condition of a rigorous test of the
586 statistical significance.

587 The main findings of our research for this topic are the following:

- 588 5. The most significant signals of solar/geomagnetic activities were obtained in the
589 drought indicator (TPPI). Because the precipitation does not respond just as well as,
590 temperatures to the solar signal, is preferred analysis TPPI variable in stead of
591 temperatures and precipitation separately.
- 592 6. From the analysis of correlations with the lags from 0 to five years delay of the
593 terrestrial variables in comparison with the solar/geomagnetic activity, we obtained



- 594 very different results, depending on the season and on the considered variables, as well
595 as on the filtering procedure. Such, we might conclude that in winter, about 2-3 years
596 after producing a maximum (minimum) solar, winter, atmospheric circulation of
597 blocking type is enhanced (weakened) over the Atlantic-European region. Also, it was
598 found that the Danube discharge in the lower basin, at the 2 or 3 years during spring
599 and summer, after a maximum (minimum) solar, will be lower (higher).
- 600 7. A terrestrial variable that respond to the solar signal, even more significant than to the
601 geomagnetic signal, is atmospheric circulation index GBO, in summer. Therefore, at
602 the 2-3 years after a maximum (minimum) of solar activity, expects a response of
603 atmospheric circulation in the Atlantic-European region, quantified by GBOI, by a
604 diminution of this index, i.e. decrease (increase) of pressure in Greenland area and an
605 increase (decrease) in atmospheric pressure in the Balkans.
 - 606 8. By multitaper method (MTM) procedure, the power spectra have highlighted both
607 quasi-periodicities related to solar activity and the other oscillations such as QBO. In
608 the time series of AEBI (spring), and EBI (winter) the most significant periodicity is
609 related to QBO (2.2-2.7 years) and with an approximately 90% confidence level there
610 are peaks at 10-14 years, which may be linked to 11-year solar cycle.
 - 611 9. The composite maps revealed that solar impact (by flux) on atmospheric circulation in
612 the middle troposphere, during the east phase of QBO, is associated with blocking
613 event over the Northern Atlantic and north-western Europe, and a geopotential with a
614 opposite distribution that occurs during the solar minimum.

615 In this study, we focused only on observational data, so that in next our investigations, we will
616 take into account significant predictors for the Danube basin found in this investigation, like
617 GBOI, TPPI and atmospheric blocking indices from the outputs of the climate simulation
618 models. Also we will take into account non-stationarities and non-linearities associated with
619 the major modes of climate variability.

620

621 *Acknowledgements.* This study has been achieved under VALUE: COST Action ES1102.

622

623 **References**

624

- 625 Barriopedro, D., Garcia-Herrera, R., and Huth, R.: Solar modulation of Northern Hemisphere
626 winter blocking, *J. Geophys. Res.*, 113, D14118, doi:10.1029/2008JD009789, 2008.
- 627 Benestad, R.E.: Schmidt GA: Solar trends and global warming, *J. Geophys. Res.* 114:D14101,
628 doi:10.1029/2008JD011639, 2009.
- 629 Blöschl, G., Nester, T., Komma, J., Parajka, J., and Perdigão, R. A. P.: The June 2013 flood in
630 the Upper Danube Basin, and comparisons with the 2002, 1954 and 1899 floods, *Hydrol.*
631 *Earth Syst. Sci.*, 17, 5197–5212, doi:10.5194/hess-17-5197-2013, 2013.
- 632 Bochníček, J., Hejda, P., and Pýcha, J.: The effect of geomagnetic and solar activity on the
633 distribution of controlling pressure formations in the Northern Hemisphere in winter,
634 *Studia geophysica et geodaetica*, 43(4), 390-398,1999.
- 635 Bretherton, C.S., Widmann, M., Dymnikov, V.P., Wallace, J.M. and Bladé, I.: The effective
636 number of spatial degrees of freedom of a time-varying field, *Journal of climate*, 12(7),
637 1990-2009, 1999.
- 638 Brugnara, Y., Brönnimann, S., Luterbacher, J., and Rozanov, E.: Influence of the sunspot
639 cycle on the Northern Hemisphere wintertime circulation from long upper-air data sets,
640 *Atmos. Chem. Phys.*, 13, 6275-6288, doi:10.5194/acp-13-6275-2013, 2013.
- 641 Cubasch, U., Voss, R., Hegerl, G.C., Waszkewitz, J. and Crowley, T.J.: Simulation of the
642 influence of solar radiation variations on the global climate with an ocean-atmosphere
643 general circulation model, *Climate Dynamics*, 13(11), 757-767, 1997.



- 644 Davini, P., Cagnazzo, C. Gualdi, S. and Navarra, A.: Bidimensional Diagnostics, Variability,
645 and Trends of Northern Hemisphere Blocking, *J. Climate*, 25, 6496–6509, 2012.
- 646 Demetrescu, C. and Dobrica, V.: Signature of Hale and Gleissberg solar cycles in the
647 geomagnetic activity, *J. Geophys. Res.*, 113, A02103, doi:10.1029/2007JA012570, 2008.
- 648 Dima, M., Lohmann, G. and Dima I.: Solar-Induced And Internal Climate Variability at
649 decadal time scales, *Int. J. Climatol.*, 25: 713–733, 2005.
- 650 Dobrica, V., C. Demetrescu, Boroneant, C. and Maris G.: Solar and geomagnetic activity
651 effects on climate at regional and global scales: Case study—Romania, *J. Atmos. Sol.-Terr.
652 Phy.*, 71 (17-18), 1727-1735, doi:10.1016/j.jastp.2008.03.022, 2009.
- 653 Dobrica V, Demetrescu, C.: On the evolution of precipitation in Central and South-Eastern
654 Europe and its relationship with Lower Danube discharge, in: AGU Fall Meeting
655 Abstracts, 11, 1030, 2012.
- 656 Drobyshev, I., Niklasson, M., Linderholm, H.W., Seftigen, K., Hickler, T., Eggertsson, O.:
657 Reconstruction of a regional drought index in southern Sweden since AD 1750, *The
658 Holocene* 21(4) 667-679, doi: 10.1177/0959683610391312, 2011.
- 659 Ebisuzaki, W.: A Method to Estimate the Statistical Significance of a Correlation when the
660 Data is Serially Correlated, *J. Climate*, 10:2147–2153, 1997.
- 661 Echer, M. S., Echer, E., Nordemann, D. J. R., and Rigozo, N. R.: Multi-resolution analysis of
662 global surface air temperature and solar activity relationship, *Journal of Atmospheric and
663 Solar-Terrestrial Physics*, 71(1), 41-44, 2009.
- 664 Echer, M.S., Echer, E., Rigozo, N.R., Brum, C.G.M., Nordemann, D.J.R., and Gonzalez,
665 W.D.: On the relationship between global, hemispheric and latitudinal averaged air surface
666 temperature (GISS time series) and solar activity, *Journal of Atmospheric and Solar-
667 Terrestrial Physics*, 74, pp.87-9, 2012.
- 668 El-Janyani, S., Massei, N., Dupont, J.P., Fournier, M. and Dörfliger, N.: Hydrological
669 responses of the chalk aquifer to the regional climatic signal, *Journal of Hydrology*, 464,
670 485-493, 2012.
- 671 Ghil, M., Allen, M.R., Dettinger, M.D., Ide, K., Kondrashov, D., Mann, M.E., Robertson,
672 A.W., Saunders, A., Tian, Y., Varadi, F., Yiou, P.: Advanced spectral methods for
673 climatic time series, *Reviews of Geophysics* 40 (1), doi: 10.1029/2001RG000092, 2002.
- 674 Gray, L. J., A. A. Scaife, D. M. Mitchell, S. Osprey, S. Ineson, S. Hardiman, N. Butchart, J.
675 Knight, R. Sutton, and Kodera K.: A lagged response to the 11 year solar cycle in observed
676 winter Atlantic/Euro pean weather patterns, *J. Geophys. Res. Atmos.*, 118, 13, 405–13,
677 420, doi:10.1002/2013JD020062, 2013.
- 678 Hertig, E., Beck, C., Wanner, H., Jacobeit, J.: A review of non-stationarities in climate
679 variability of the last century with focus on the North Atlantic-European sector, *Earth-
680 Science Reviews* 147, 1–17, doi:10.1016/j.earscirev.2015.04.009, 2015.
- 681 Hurrell, J.W., Kushnir Y, Visbeck M, Ottersen G: Research Abstracts EGU2007-A-08910
682 9:1029- 2003. An overview of the North Atlantic Oscillation. In: Hurrell, J.W., Kushnir,
683 Y., Ottersen, G., Visbeck, M. (Eds.), *The North Atlantic Oscillation, Climatic Significance
684 and Environmental Impact*, AGU Geophysical Monograph, 134, 1–35, 2003.
- 685 Huth, R., Pokorná, L., Bochniček, J., and Hejda, P.: Combined solar and QBO effects on the
686 modes of low-frequency atmospheric variability in the Northern Hemisphere, *Journal of
687 Atmospheric and Solar-Terrestrial Physics*, 71(13), 1471-1483, 2009.
- 688 Lejenas, H., and Okland, H.: Characteristics of Northern Hemisphere blocking as determined
689 from a long time series of observational data, *Tellus*, 35A, 350-362, 1983.
- 690 Lohmann, G., Rambu, N., and Dima, M.: Climate signature of solar irradiance variations:
691 analysis of long-term instrumental, historical, and proxy data, *International Journal of
692 Climatology*, 24(8), pp.1045-1056, 2004.



- 693 Love, J. J., K. Mursula, V. C. Tsai, and Perkins, D. M.: Are secular correlations between
694 sunspots, geomagnetic activity, and global temperature significant?, *Geophys. Res. Lett.*,
695 38, L21703, doi: 10.1029/2011GL049380, 2011.
- 696 Mann, M. E. and Lees, J.: Robust estimation of background noise and signal detection in
697 climatic time series, *Climatic Change*, 33, 409–445, 1996.
- 698 Mann, M. E.: On smoothing potentially non-stationary climate time series, *Geophys. Res.*
699 *Lett.*, 31, L07214, doi: 10.1029/2004GL019569, 2004.
- 700 Mann, M. E.: Smoothing of climate time series revisited, *Geophys. Res. Lett.*, 35, L16708,
701 doi: 10.1029/2008GL034716, 2008.
- 702 Mares, I., Mares, C., Mihailescu, M.: NAO impact on the summer moisture variability across
703 Europe, *Physics and chemistry of the Earth*, 27, 1013-1017, 2002.
- 704 Mares C., Mares, I., and Stanciu, A.: On the possible causes of the severe drought in the
705 Danube lower basin in 2003, in: Proceedings of the International Conference on "Water
706 Observation and Information System for Decision Support" Ohrid, Republic of
707 Macedonia, 23- 26 May., 2006.
708 http://balwois.mpl.ird.fr/balwois/administration/full_paper/ffp-672.pdf)
- 709 Mares, C., Mares, I. and Stanciu, A.: Extreme value analysis in the Danube lower basin
710 discharge time series in the 20th century, *Theoretical and Applied Climatology*, 95, 223-
711 233, 2009.
- 712 Mares, I., Mares, C., Stanciu, A., and Mihailescu, M.: On the climate models performances to
713 simulate the main predictors that influence the discharges in the Danube middle and lower
714 basin, *Geophysical Research Abstracts*, 13, EGU2011-2325, EGU General Assembly,
715 2011.
- 716 Mares, C., Mares, I. Stanciu, A., and Mihailescu, M.: North Atlantic Oscillation (NAO)
717 influence on the Danube lower basin, *Proc. Fifth Int. Scientific Conf. on Water, Climate
718 and Environment: BALWOIS 2012*, Ohrid, Macedonia, Balwois, 2012-771, 2012.
- 719 Mares, I., Mareş, C. and Mihăilescu M.: On the statistical significance of the sea level
720 pressure climatic signal simulated by general circulation models for the 21st century over
721 Europe. *Rev. Roum. Géophysique*, 25–40, 2013a.
- 722 Mares, I., Mareş, C., and Mihailescu, M.: Stochastic modeling of the connection between sea
723 level pressure and discharge in the Danube lower basin by means of Hidden Markov
724 Model, *EGU General Assembly Conference Abstracts*, 15, 7606, 2013b.
- 725 Mares, I., Dobrica, V., Demetrescu, C. and Mares, C.: Moisture variability in the Danube
726 lower basin: an analysis based on the Palmer drought indices and the solar/geomagnetic
727 activity influence, *Geophysical Research Abstracts*, 16, EGU2014-6390, 2014.
- 728 Mares, C., Adler M. J., Mares I, Chelcea, S., Branescu, E.: Discharge variability in
729 Romania using Palmer indices and a simple atmospheric index of large-scale circulation,
730 *Hydrological Sciences Journal*, doi: 10.1080/02626667.2015.1006233), 2015a.
- 731 Mares, I., Dobrica, V., Demetrescu, C., and Mares, C.: Influence of the atmospheric blocking
732 on the hydrometeorological variables from the Danube basin and possible response to the
733 solar/geomagnetic activity, *Geophysical Research Abstracts*, 17, EGU2015-4154-3, 2015,
734 EGU General Assembly 2015 (PICO2.6), 2015b.
- 735 Mares, C., Mares, I., and Mihailescu, M.: Identification of extreme events using drought
736 indices and their impact on the Danube lower basin discharge, *Hydrological Processes*,
737 doi: 10.1002/hyp.10895), 2016a.
- 738 Mares, I., Dobrica, V. Demetrescu, C., and Mares, C.: Hydrological response in the Danube
739 lower basin to some internal and external forcing factors of the climate system,
740 *Geophysical Research Abstracts*, 18, EGU2016-7474, EGU General Assembly 2016b.
741



- 742 Massei, N., Laignel, B., Deloffre, J., Mesquita, J., Motelay, A., Lafite, R., and Durand, A.:
743 Long-term hydrological changes of the Seine River flow (France) and their relation to the
744 North Atlantic Oscillation over the period 1950–2008, *International journal of*
745 *Climatology*, 30(14), pp.2146-2154, 2010.
- 746 Palamara, D.R. and Bryant, E.A.: March. Geomagnetic activity forcing of the Northern
747 Annular Mode via the stratosphere, in: *Annales Geophysicae*, 22, No. 3, 725-731, 2004
- 748 Papadimitriou, L. V., Koutroulis, A. G., Grillakis, M. G., and Tsanis, I. K.: High-end climate
749 change impact on European runoff and low flows – exploring the effects of forcing biases,
750 *Hydrol. Earth Syst. Sci.*, 20, 1785-1808, doi:10.5194/hess-20-1785-2016, 2016.
- 751 Press, W. H., S. A. Teukolsky, W. T. Vetterling, and Flannery, B. P.: *Numerical Recipes*,
752 Cambridge Univ. Press, Cambridge, U. K., 1992
- 753 Prestes, A., Rigozo, N. R., Nordemann, D. J. R., Wrasse, C. M., Echer, M. S., Echer, E., ...
754 and Rampelotto, P. H.: Sun–earth relationship inferred by tree growth rings in conifers
755 from Severiano De Almeida, Southern Brazil, *Journal of Atmospheric and Solar-*
756 *Terrestrial Physics*, 73(11), 1587-1593, 2011.
- 757 Rimbu N, Boroneanț C, Buță C, and Dima M.: Decadal variability of the Danube river flow
758 in the lower basin and its relation with the North Atlantic Oscillation, *International Journal*
759 *of Climatology*., 22(10):1169-79, 2002.
- 760 Rimbu, N., and Lohmann, G.: Winter and summer blocking variability in the North Atlantic
761 region—evidence from long-term observational and proxy data from southwestern
762 Greenland, *Climate of the Past*, 7(2), 543-555, 2011.
- 763 Rimbu, N., Dima, M., Lohmann, G. and Musat, I.: Seasonal prediction of Danube flow
764 variability based on stable teleconnection with sea surface temperature, *Geophysical*
765 *Research Letters*, 32(21), 2005.
- 766 Scaife, A. A., Ineson, S., Knight, J. R., Gray, L.J., Kodera, K., and Smith, D. M.: A
767 mechanism for lagged North Atlantic climate response to solar variability, *Geophys. Res.*
768 *Letts.*, 40, 434–439, doi:10.1002/grl.50099, 2013.
- 769 Sfică, L., Voiculescu, M., and Huth, R.: The influence of solar activity on action centres of
770 atmospheric circulation in North Atlantic, *Ann. Geophys.*, 33, 207-215,
771 doi:10.5194/angeo-33-207-2015, 2015.
- 772 Thiebaut, H. J., and Zwiers, F. W.: The interpretation and estimation of effective sample size,
773 *J. Climate Appl. Meteor.*, 23, 800–811, 1984.
- 774 Thomson, D. J.: Spectrum estimation and harmonic analysis, *IEEE Proc.*, 70, 1055-1096,
775 1982.
- 776 Torrence, C., and Compo, G. P.: A practical guide to wavelet analysis. *Bull. Amer. Meteor.*
777 *Soc.*, 79, 61–78, 1998.
- 778 Trenberth, K. E., and Paolino, D. A.: The Northern Hemisphere sea level pressure data set:
779 Trends, errors, and discontinuities, *Mon. Weather Rev.* 108: 855-872, 1980.
- 780 Turki, I., Laignel, B., Massei, N., Nouaceur, Z., Benhamiche, N., and Madani, K.:
781 Hydrological variability of the Soummam watershed (Northeastern Algeria) and the
782 possible links to climate fluctuations, *Arabian Journal of Geosciences*, 9(6), 1-12, 2016.
- 783 Valty, P., De Viron, O., Panet, I., and Collilieux, X.: Impact of the North Atlantic Oscillation
784 on Southern Europe Water Distribution: Insights from Geodetic Data. *Earth*
785 *Interactions*, 19(10), 1-16, 2015.
- 786 Van Loon H. and Labitzke, K: Association between the 11-Year Solar Cycle, the QBO, and
787 the Atmosphere. Part II: Surface and 700 mb in the Northern Hemisphere in Winter, *J.*
788 *Climate*, 1, 905–920, 1988.
- 789 Van Loon, H., and Meehl, G. A.: Interactions between externally forced climate signals from
790 sunspot peaks and the internally generated Pacific Decadal and North Atlantic Oscillations,
791 *Geophys. Res. Lett.*, 41, 161–166, doi:10.1002/ 2013GL058670, 2014.



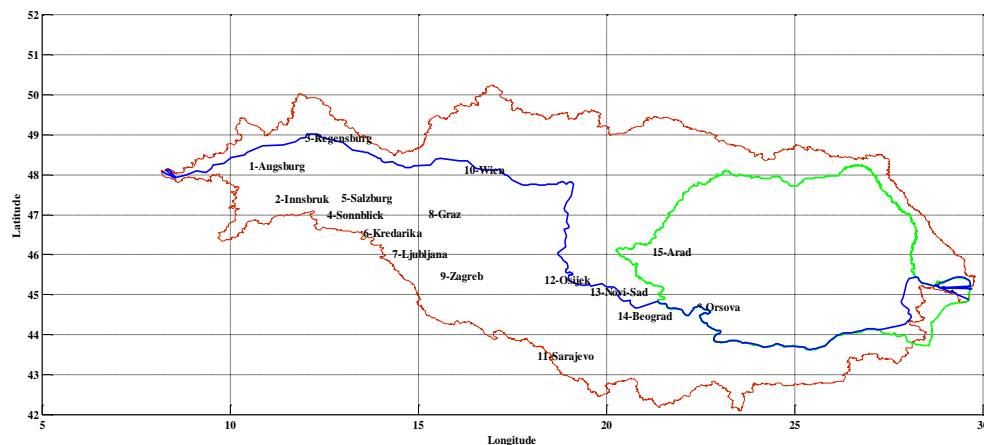
Correlation with Wolf number							
PC1_TT(4-8)	Summer	0.288	2.453	0.157	0.021	68	98%
PC1_TT(9-15)	Fall	0.699	3.770	0.550	0.000	17	99.5%
PC1_PP(4-8)	Spring	-0.242	2.133	-0.190	0.005	75	95-98%
PC1_PP(9-15)	Spring	-0.538	2.417	-0.363	0.000	16	95-98%
PC1_PP(4-8)	Winter	-0.370	3.298	-0.265	0.000	70	>99%
TPPI(UF)	Spring	0.211	1.973	0.148	0.029	85	95%
TPPI(LPF)	Spring	0.299	1.736	0.261	0.000	33	90%
TPPI(4-8)	Spring	0.245	2.154	0.159	0.019	74	95-98%
TPPI(9-15)	Spring	0.585	2.708	0.395	0.000	16	98%
TPPI(9-15)	Fall	0.673	3.796	0.553	0.000	19	99%
GBOI (4-8)	Summer	-0.346	2.982	-0.230	0.001	67	99.5%
GBOI (4-8)	Winter	-0.343	3.169	-0.218	0.001	77	>99%
GBOI (17-28)	Fall	-0.899	3.485	-0.707	0.000	5	95-98%
Q_ORIS (4-8)	Winter	-0.263	2.329	-0.163	0.016	75	98%

816
 817
 818
 819

Table 3. Same as Table 2 but for 53 years (1948-2000).

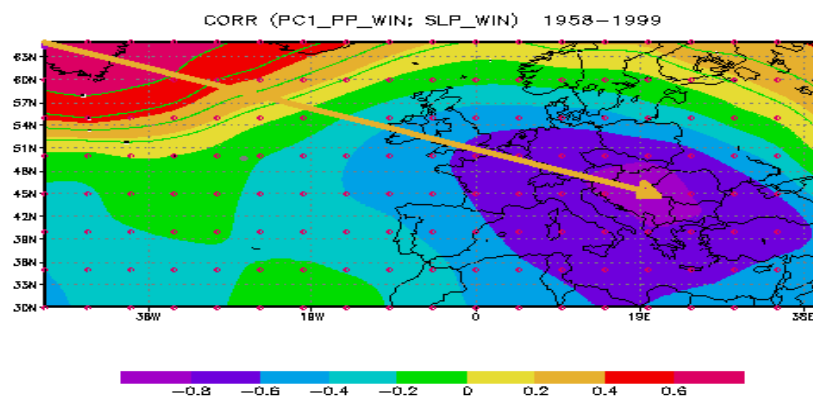
Variable	Season	r	t	τ	p	N_{eff}	CL
Correlation with aa							
EBI (UF)	Spring	0.259	1.836	0.151	0.110	49	~95%
EBI (4-8)	Spring	0.528	3.864	0.382	0.000	41	>99%
ABI (UF)	Fall	-0.257	1.848	-0.118	0.210	51	~95%
ABI (9-15)	Spring	0.605	2.157	0.426	0.000	10	>95%
AEBI (9-15)	Winter	0.749	3.134	0.589	0.000	10	98.5%
Correlation with flux 10.7 cm							
TPPI(LPF)	Spring	0.444	1.502	0.322	0.001	11	85-90%
ABI(4-8)	Fall	0.578	4.124	0.312	0.001	36	99.9%
AEBI(4-8)	Fall	0.530	3.697	0.360	0.000	37	99.9%
EBI (4-8)	Winter	0.419	2.678	0.272	0.004	37	98.5%
Q_ORIS(4-8)	Winter	-0.603	4.390	-0.351	0.000	36	99.9%
GBOI (4-8)	Winter	-0.695	6.034	-0.428	0.000	41	99.9%

820
 821



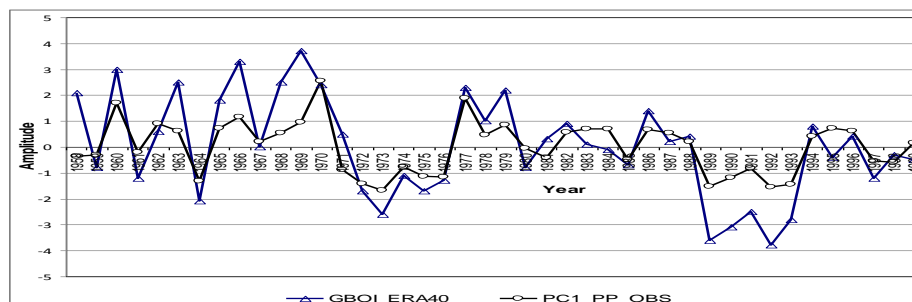
822
 823

Figure 1. Localization of 15 precipitation stations situated upstream of Orsova station.



824
 825
 826
 827
 828
 829

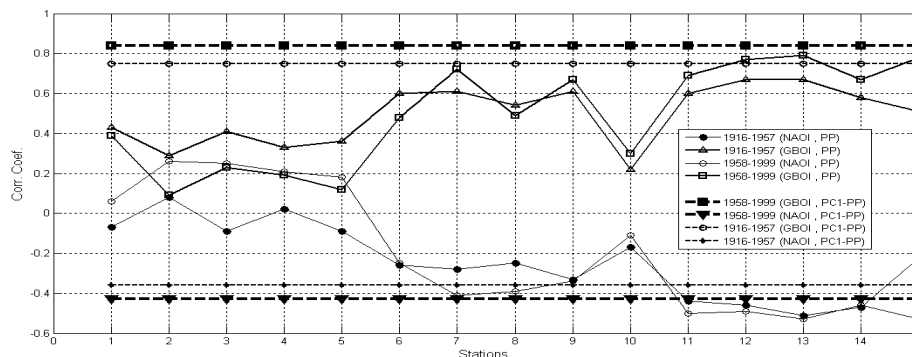
Figure 2. Spatial distribution of correlation coefficients between SLP NCAR and observed PC1- PP during winter for 1958-1999.



830

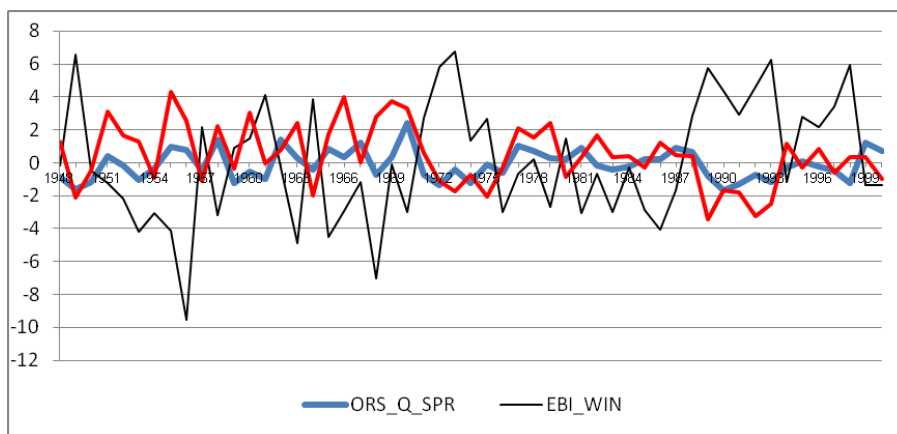
Figure 3. Winter precipitation PC1 versus winter GBOI for 1958-1999 ($R=0.84$).

832
 833



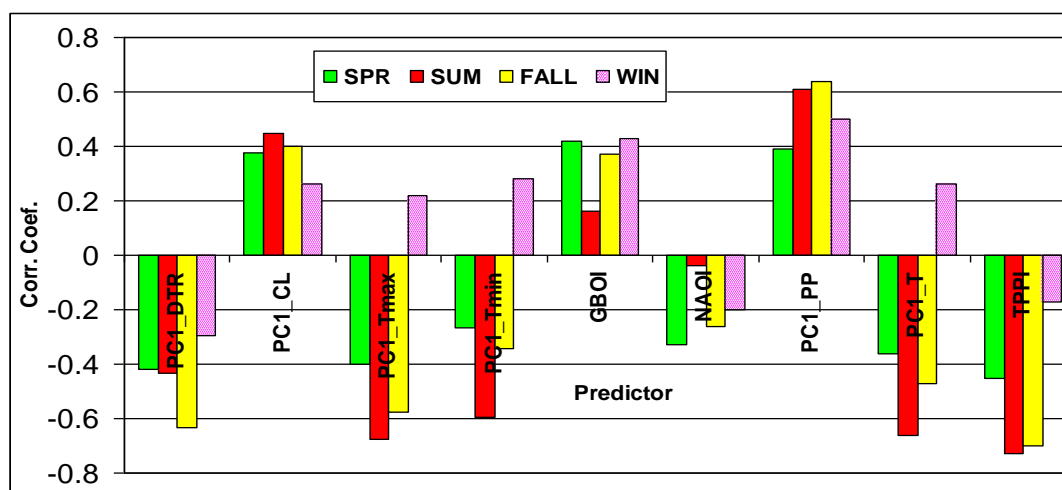
834
 835
 836
 837

Figure 4. Correlation coefficients between winter precipitation at 15 stations and NAOI and GBOI for two periods: a) 1916-1957; b) 1958-1999. The correlations between PC1-PP and two indices are marked by horizontal lines.



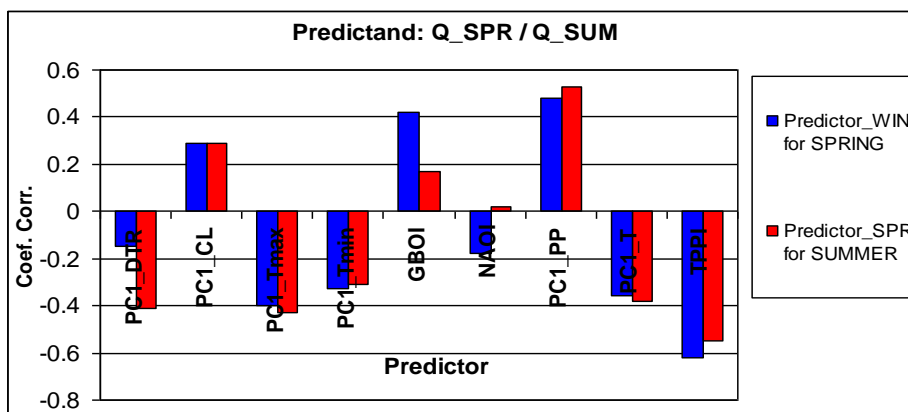
838
 839
 840
 841
 842
 843
 844
 845

Figure 5. Spring Orsova discharge versus winter European blocking index ($R = -0.54$) and winter GBOI ($R=0.53$) for the period 1948-2000.



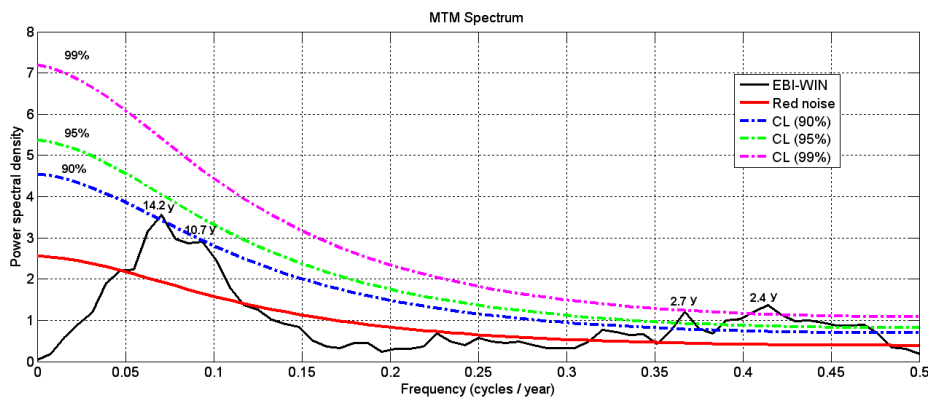
846
 847
 848
 849
 850

Figure 6. Simultaneous correlations between Danube discharge at Orsova and nine predictors (1901-2000)



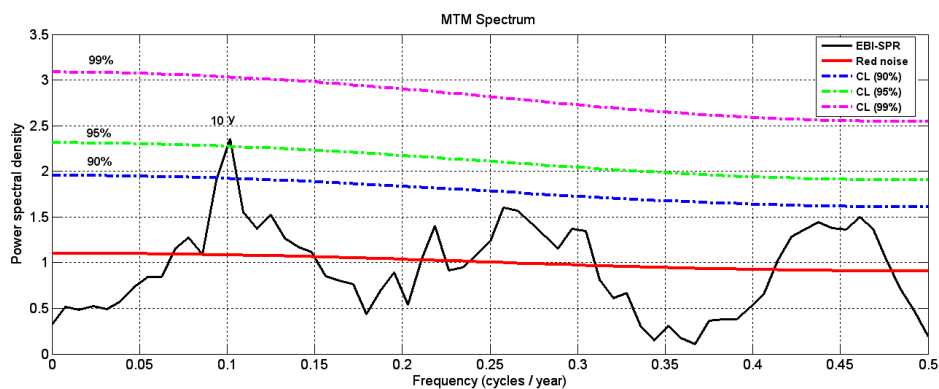
851
 852
 853
 854
 855
 856

Figure 7. The correlation between Orsova discharge (Q) in the spring / summer and the nine predictors in the winter/spring.



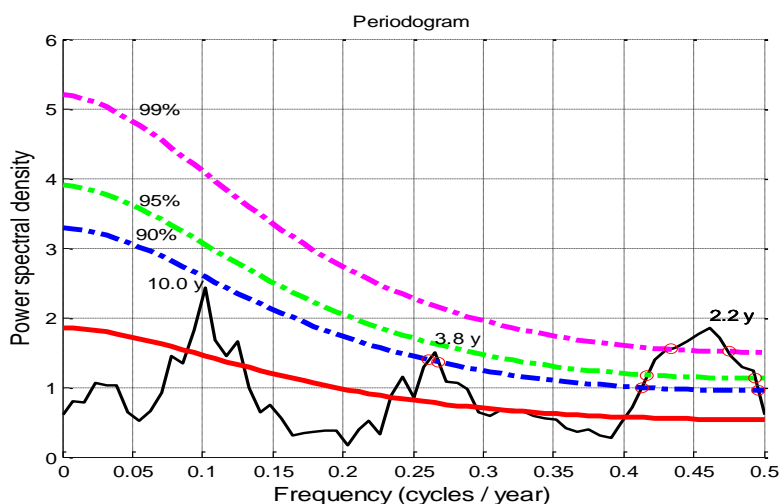
857
 858
 859

a)



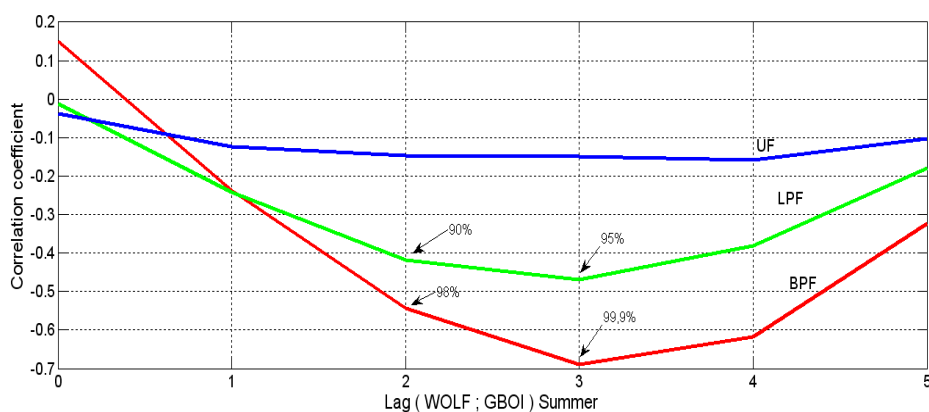
860
 861
 862

b)



863
 864
 865
 866
 867
 868
 869

c) **Figure 8.** Power spectra for the blocking indices: winter EBI (a), spring EBI (b) and spring AEBI (c).

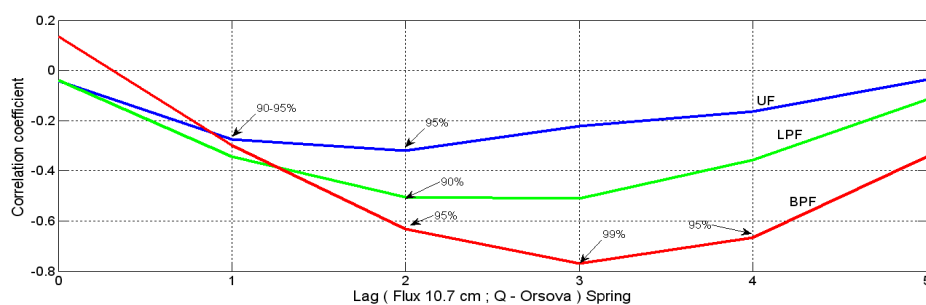


870
 871
 872
 873
 874
 875
 876
 877
 878
 879
 880
 881
 882
 883
 884

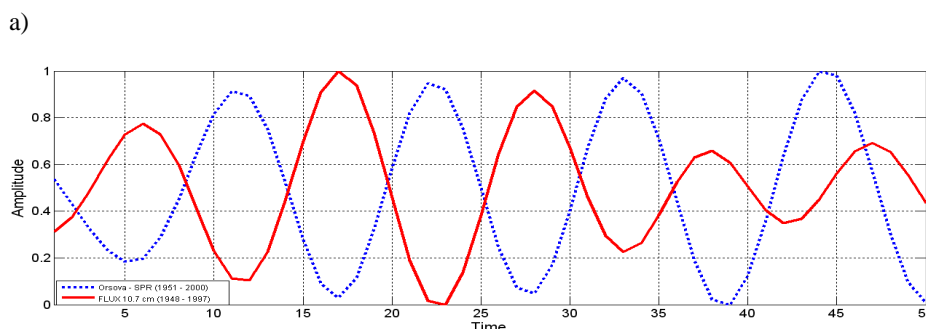
Figure 9. Correlation coefficients, between Wolf number and GBOI index in summer with the lags 0-5, for three time series: unfiltered (UF), smoothing by low pass filter (LPF) and by band pass filter (9-15)



885

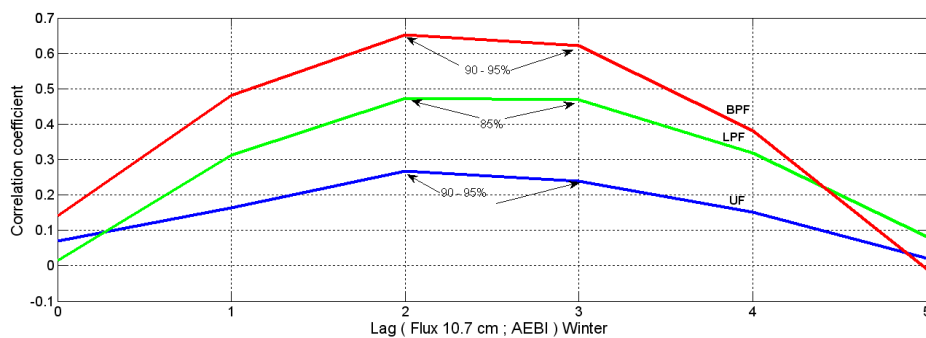


886
 887
 888



889
 890
 891
 892
 893
 894
 895
 896
 897
 898
 899

Figure 10. Solar (Flux 10.7cm) signal in the Orsova discharge (Q_{ORS}), during spring (1948-2000).
 a) Correlation coefficients, between solar flux and Orsova discharge with the lags 0-5, for three time series: unfiltered (UF), smoothing by low pass filter (LPF) and by band pass filter (9-15);
 b) Temporal behavior of the solar flux and Q_{ORS} , filtered (9-15) with a delay of 3 years to flux. The time series are normalized.

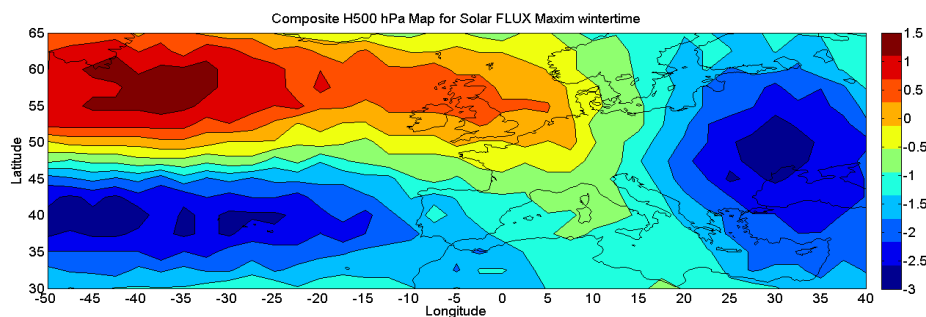


900
 901
 902
 903
 904
 905
 906
 907
 908

Figure 11. Correlation coefficients, between solar flux and AEBI with the lags 0-5, during winter (1948-2000), for three time series: unfiltered (UF), smoothing by low pass filter (LPF) and by band pass filter (9-15).



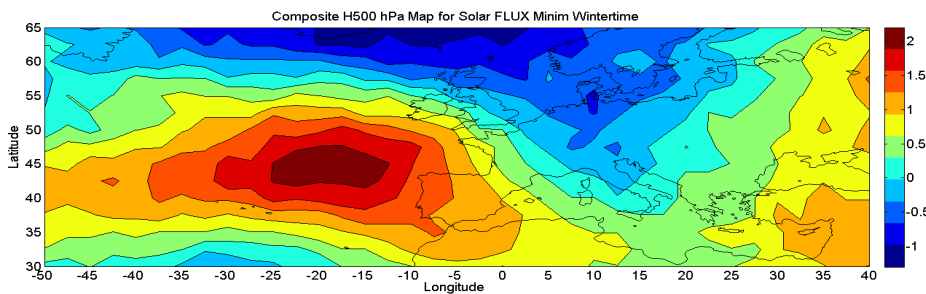
909



910

a)

912



913

914

915

916

917

918

Figure 12. Composite maps for the winter H500 hPa anomalies, corresponding to solar flux associated with the east phase of QBO (1948-2000) and: a) maximum flux b) minimum flux